MATHEMATICAL BIOSCIENCES
AND ENGINEERING
Volume **11**, Number **3**, June **2014**

doi:10.3934/mbe.2014.11.667

pp. **667–677**

MATHEMATICAL MODELING OF GLASSY-WINGED SHARPSHOOTER POPULATION

Jeong-Mi Yoon and Volodymyr Hrynkiv

Department of Mathematics and Statistics
University of Houston - Downtown
Houston, TX 77002, USA

Lisa Morano

Department of Natural Sciences
University of Houston - Downtown
Houston, TX 77002, USA

Anh Tuan Nguyen and Sara Wilder

University of Houston - Downtown
Houston, TX 77002, USA

Forrest Mitchell

Department of Entomology
Texas A&M AgriLife Research
Stephenville, TX 76401, USA

(Communicated by Yang Kuang)

Abstract. Pierce's disease (PD) is a fatal disease of grapevines which results from an infection by the plant pathogen *Xyllela fastidiosa*. This bacterium grows in the xylem (water-conducting) vessels of the plant blocking movement of water. PD can kill vines in one year and poses a serious threat to both the California and the expanding Texas wine industries. Bacteria are vectored from one vine to the next by a number of xylem feeding insect species. Of these, the Glassy-winged Sharpshooter (GWSS) is considered to be the primary xylem feeding insect in Texas vineyards. An extensive database of the xylem-feeding population frequencies was collected by USDA-APHIS for Texas vineyards over multiple years. This project focused on a subset of data, GWSS frequencies within 25 vineyards in Edwards Plateau located in central Texas. The proposed model investigates the natural population dynamics and the decline in GWSS, likely the result of pest management campaigns on the insects within the region. The model is a delay Gompertz differential equation with harvesting and immigration terms, and we use the data to estimate the model parameters.

1. **Introduction.** *Xylella fastidiosa* (Wells) (*Xf*) (Wells et al. 1983) is a Gram negative bacterium which infects the xylem of both native vegetation and agricultural crops. There are strains of *Xf* which invade native Texas shrubs and annual plants with no apparent disease symptoms, but there are numerous *Xf* strains which invade agricultural hosts including almond, oleander, citrus, and grapes. When *Xf* infects

2010 *Mathematics Subject Classification.* Primary: 92D25, 92D40; Secondary: 93C23.
Key words and phrases. Mathematical modeling, Pierce's disease, Glassy-winged sharpshooter.

varieties of the European grape species *Vitis vinifera* (Cabernet Sauvignon, Merlot, etc.) it causes Pierce's Disease (PD) [13]. PD in grapes results in the blocking of xylem, slow in water transport and ultimately the death of grapevines (Hopkins 1989). *Xf* is vectored from plant to plant by xylem feeding insects. The primary PD vector is known as the Glassy-winged Sharpshooter (GWSS), *Homalodisca vitripennis* (Germar) (Hemiptera: Cicadellidae), formerly *H. coagulata* [23, 28]. PD is not only pathogenic it is a financially dangerous disease for growers as it can kill a vineyard within 1-2 years. PD outbreaks can therefore have a crippling effect on the California and Texas wine industries.

Serious outbreaks of PD occurred in California in the late 1990s. These outbreaks and the realization that the population of GWSS vectoring the disease in California was originally from Texas [7], led the USDA-APHIS to fund PD research in both California and Texas. Texas AgriLife Research worked to compile a database of the insects found in Texas vineyards. Forty vineyards participated in the insect collection; each placing 4 to 5 traps within their vineyards continuously from 2003 to 2010. Identification of all sharpshooters on every trap collected every two weeks for years resulted in an enormous data set of insect frequencies (almost 48K rows of data).

Studies of the GWSS have resulted in improved understanding of how easily the insect can invade vineyards and transmit PD. The GWSS is known to feed on a diverse collection of plant host species which allows it to have continuous food supply as it moves into new areas. If growing in a warm area the GWSS typically has a 3 month maturation period and 2 hatching cycles [3, 15, 25]. The first generation of insects usually matures by May. This generation lays eggs which can grow up and result in a smaller second generation of GWSS that can then hatch between June - September. This second generation of sharpshooters can be quite dangerous spreading *Xf* to multiple other vines because bacterial levels are higher within plants later in the season.

An initial statistical treatment of the large Texas data set also showed that the GWSS had the greatest frequencies across Texas and was the most ecologically flexible [22]. Statistical analysis of the enormous USDA-APHIS data set resulted in several specific findings. We determined that there were clearly three top species of xylem-feeding insects in Texas based on their greatest frequencies on traps and these included the sunflower spittle bug, *Clastoptera xanthocephala* (Germar), a smaller green sharpshooter, *Graphocephala versuta* (Say), and the larger brown GWSS, *H. vitripennis*. Using canonical correspondence analysis we were able to show that the three insect species distributed significantly ($p = 0.001$) along environmental gradients with *G. versuta* showing greater abundance in wetter ecoregions, the spittlebug showing greater numbers at higher elevations and the GWSS showing no correlation with any particular ecoregions [22].

The goal of this study was to create a model of the GWSS population dynamics from multiple vineyards over a time period of years. The model would need to address the annual oscillations in the insect populations and incorporate how these populations changed over a long time scale. The years covered in this study start from a time when the insects were at high levels and follow the populations as growers and extension experts worked to reduce the dangerous populations of GWSS. Rarely in biology is there such an extensive population data set to be analyzed which also spans such a long time period (with respect to the life span of the organism). This data set also comes from the field where little can be controlled

(unlike laboratory experiments). As such, creating a model of real insect data would allow for us to predict not only the annual cycle of insect hatchings, but a way to model the impact of educational, viticultural and chemical interventions to reduce insect populations within an agricultural industry.

2. **The data.** We focused this mathematical model of GWSS frequencies on a region of Texas known as Edwards Plateau of the Texas Hill Country. We started with a USDA-APHIS data set of insect trapped in up to forty vineyards throughout Texas. The resulting data set was an excel sheet, 47,828 rows by 42 columns, detailing the conditions of every trap in every vineyard from 2003 to 2010 continuously. By focusing on just the Texas Hill County region which contained 25 vineyards and is the densest viticulture area in Texas, we hoped to reduce the noise in insect numbers created by differences in soil, eco-region or weather. The frequency of each trap was divided by the total trapping days to achieve an average daily frequency for each trap. Insect counts were summed for all traps for the region. Histograms were then created to view total number of insects per day over time. The vertical axis is the sum of GWSS for all vineyards in the study per day. These totals are assumed to be proportional to the number of insects in the area.

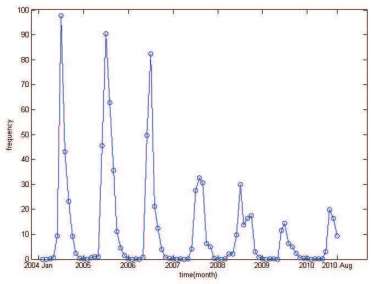

FIGURE 1. Histogram of GWSS in Central Texas

3. **Model.** To fit the experimental data shown in Figure 1 we consider a delay differential equation with harvesting and immigration. Various types of delay differential equations have been used by many researchers in mathematical modeling to take into account gestation periods, feeding times, reaction times, etc. The reader is referred to [6, 10, 16, 18, 20, 24] for a more detailed discussion of many different delayed biological systems. In population dynamics, the growth rate R in a single species model is usually a function of the population N. One possible general form of such an equation without harvesting and immigration is as follows

$$\frac{dN}{dt} = N(t)R(N(t-\tau)). \tag{1}$$

The delay $\tau > 0$ accounts for factors such as gestation time, hatching period, renewal of food, etc. [4]. It is suitable for modeling population growth in our case, since hatching/maturation must occur to increase the population size. Thus the time delay τ in equation (1) can be interpreted as the hatching/maturation period for the population. We use equation (1) (where the rate of growth R will be specified

soon) to model temporal dynamics of the insect population. If, in addition, we introduce harvesting and immigration, then (1) takes the form

$$\frac{dN}{dt} = N(t)R(N(t-\tau)) - cN(t) + I, \tag{2}$$

where for simplicity we assume that $c > 0$ and I are real numbers. Harvesting and immigration terms take into account the controlling factors such as pesticide use, information and education campaigns, weed management, etc. If one chooses $R = r(1 - \frac{N(t)}{K})$ then equation (1) represents a logistic growth, where K is a carrying capacity, and in this case it is called Hutchinson-Wright equation [14, 30, 16].

For our model, we choose the Gompertz growth

$$R = -r \ln \frac{N(t)}{K}.$$

The Gompertz curve has a sigmoid shape (just like the logistic growth) but it is asymmetric about its point of inflection. As a result, in comparison to the logistic curve, it exhibits faster growth at the beginning, slows down as the resources become limited, and stabilizes faster on the carrying capacity. These features together with the biology of the insect motivated us to use the Gompertz curve for the growth rate R since a model with a sharper rate of increase (Gompertz) would be a more realistic one. It also fit our real world data better than the logistic growth. The Gompertz growth has been used to model the growth of plants, tumors as well as fish population [5, 29, 9]. All in all, we consider the following model

$$\frac{dN}{dt} = -rN(t) \ln \frac{N(t-\tau)}{K} - cN(t) + I, \tag{3}$$

supplemented with an initial condition which has to be specified on an entire interval of length τ

$$N(t) = N_0(t), -\tau \le t \le 0. \tag{4}$$

For the sake of computational convenience, in our simulations we choose $N_0(t) = 1$. Table 1 below provides the information about the meaning of the parameters.

Table 1. Meaning of the parameters for (3)

Parameter	Meaning	Units
τ	time delay	month
K	carrying capacity	number of insects
r	intrinsic rate of growth	1/month
c	harvesting effort	1/month
I	immigration rate	number of insects/month

- For the numerical simulations in section 5 we chose $\tau = 3.05$, since in warm areas the insects will lay eggs in February and they will hatch and go through a series of nymph stages before they become adults in late May [3, 15, 25]. This typical cycle from egg to adult takes about 3 months in the spring and so this value of slightly over 3 months was used.
- There is evidence [11, 15, 17, 23] that numerous items can cause a population explosion of the insect vector. These may be preferred temperatures or planting of high amounts of appropriate plant material (lots of grapevines or weeds around vineyards which host the insects), good water levels in the plant material, invasion of a new insect or insect population and lack of predators. At the time when this data was being collected there was clearly a very high explosion of the insect population every spring. Although it is unclear what

caused the high levels, it appeared that the education campaign to growers, use of insecticide and/or particular weather patterns started to bring the insects down. We assumed that the numbers to which the insects were lowered (with all controls in place) were close to the normal carrying capacity K of the system and estimated $K = 16$ from the histogram.

- Value $r = 0.52$ was chosen as the approximate value given for a common field grasshopper as a function of eggs produced per original individual per development across several immature stages [2].

4. **Stability analysis.** We rewrite (3) as follows

$$\frac{dN}{dt} = F(N(t), N(t-\tau)), \tag{5}$$

where $F(N(t), N(t-\tau)) := -rN(t)\ln\frac{N(t-\tau)}{K} - cN(t) + I$. We see that equilibrium point(s) $F(N^*(t), N^*(t-\tau)) = 0$ of (5) can be found only numerically. To verify the feasibility of the model we graph N^* as a function of c (see Figure 2). We see from Figure 2 that as the efforts to eliminate the insect are increased the number of insects declines to a negligible number which makes sense biologically.

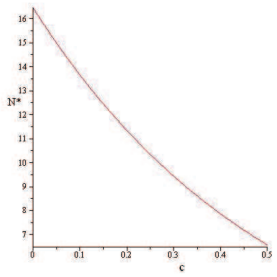

FIGURE 2. Graph of N^* as a function of c with $K = 16, r = 0.52, \tau = 3.05, I = 0.24$.

To determine stability of equilibria we linearize equation (5) around the equilibrium point N^*. To this end, we introduce a new variable $x(t) = N(t) - N^*$ and linearize

$$\frac{dx(t)}{dt} = \frac{\partial F}{\partial N(t)}\Big|_{N=N^*} x(t) + \frac{\partial F}{\partial N(t-\tau)}\Big|_{N=N^*} x(t-\tau),$$

to get

$$\frac{dx(t)}{dt} = Ax(t) + Bx(t-\tau), \tag{6}$$

where $A = -c - r\ln(N^*/K)$ and $B = -r$. By rescaling time ($\tilde{t} = t/\tau$), equation (6) can be rewritten in the following form

$$\frac{dx(\tilde{t})}{d\tilde{t}} = ax(\tilde{t}) + bx(\tilde{t}-1), \tag{7}$$

where $a = A\tau$ and $b = B\tau$. Stability analysis of (6) (or, equivalently (7)) is well-known and has been solved completely (see, for example [12, 26, 27]). Since this

equation is linear it is reasonable to try an exponential solution $x(\tilde{t}) = Ce^{\lambda\tilde{t}}$. This gives the following transcendental equation

$$\lambda = a + be^{-\lambda}. \tag{8}$$

If we write $\lambda = \mu + i\omega$ and substitute it into the equation (8), then after careful derivation one can obtain the stability diagram for equation (7) shown in Figure 3 (see [26]). For a detailed derivation of the diagram the reader is referred to [26] as well as to [12, 27].

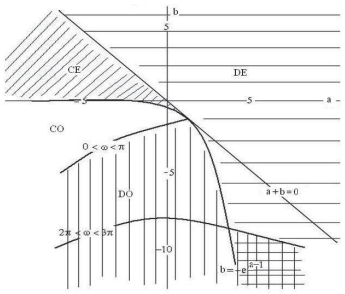

FIGURE 3. Stability boundaries for (7) (see [26]). Horizontal hatching, divergent exponential (DE); diagonal hatching, convergent exponential (CE); unhatched, convergent oscillations (CO); vertical hatching, divergent oscillations (DO).

Since our region of interest is convergent oscillations, the diagram gives us a good starting point for possible ranges of parameter values to fit the data. Another result (see [27]) is also helpful for stability considerations and we state it below.

Theorem 4.1. *In the equation* (6),
(a) if $A + B > 0$, *then* $x = 0$ *is unstable.*
(b) if $A + B < 0$ *and* $B \geq A$, *then* $x = 0$ *is asymptotically stable.*
(c) if $A + B < 0$ *and* $B < A$, *then there exists* $\tau^* > 0$ *such that* $x = 0$ *is asymptotically stable for* $0 < \tau < \tau^*$ *and unstable for* $\tau > \tau^*$, *where*

$$\tau^* = (B^2 - A^2)^{-1/2} \cos^{-1}(-A/B). \tag{9}$$

To investigate the effect of harvesting on the population dynamics, we graph A, B, and $A + B$ from (6) as a function of harvesting effort c (see Figure 4(a) and Figure 4(b)) for $K = 16, r = 0.52, \tau = 3.05$, and $I = 0.24$.

We see that $A+B < 0$ is always true and $B < A$ when $c < 2.353$. Then part (c) of Theorem 4.1 guarantees the existence of $\tau^* = (B^2 - A^2)^{-1/2} \cos^{-1}(-A/B) \approx 3.128$ such that $x = 0$ is asymptotically stable for $0 < \tau < \tau^*$ and unstable for $\tau > \tau^*$. In our case, $\tau = 3.05$ hence giving us the desired asymptotic stability. Moreover, we can use formula (9) to graph τ^* as a function of c (see Figure 5). Let c^* denote the point of intersection of the two graphs on Figure 5. Then we can find from Figure 5 that $c^* \approx 0.329$. Hence, c^* denotes a minimal harvesting effort above which the system is stabilized. Then it is clear that the graph of τ^* as a function of c^* is given by the red line in Figure 5. Practical application of the graph of τ^* as a function of c^* is that if, for some reason, the system becomes unstable (for example, due to some environmental factors, etc.), then we can find a minimal level of harvesting effort c^* at which the system is stabilized. The minimality of effort is important since cost is included in harvesting.

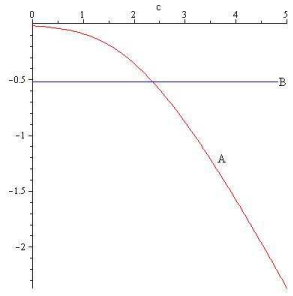

(a) A and B as a function of c

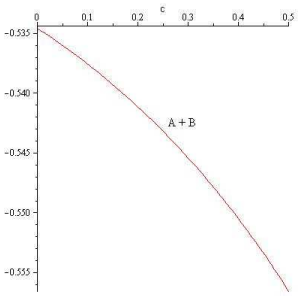

(b) $A + B$ as a function of c

FIGURE 4. $K = 16, r = 0.52, \tau = 3.05$, and $I = 0.24$.

Qualitatively, this minimal harvesting effort c^* can be also seen from the stability diagram in Figure 3. That is, if we pick a point in any unstable part of the diagram in Figure 3, then by changing c appropriately, we change only $a-$coordinate (because the $b-$coordinate does not depend on c) hence driving our system to stability.

5. **Numerical simulation.** Using biological considerations, Figure 3, and Theorem 4.1, we determined that the following values of $r = 0.52$, $K = 16.0$, $\tau = 3.05$, $0.25 \leq c \leq 0.45$, and $0.15 \leq I \leq 0.4$ give a reasonable visual fit to the data. Then using these values as a basis we simulated the model to determine optimal values of parameters c and I. To determine the optimal parameter values compared to the real data, we define an error function as follows

$$\begin{aligned} Error = &\frac{1}{\sqrt{2\pi}}\Big(\sum_{i=1}^{12}(N-N_i)^2 e^{-\frac{(N-6)^2}{2}} + \sum_{i=13}^{24}(N-N_i)^2 e^{-\frac{(N-18)^2}{2}} + \ldots \\ &+ \sum_{i=85}^{92}(N-N_i)^2 e^{-\frac{(N-90)^2}{2}}\Big), \end{aligned} \tag{10}$$

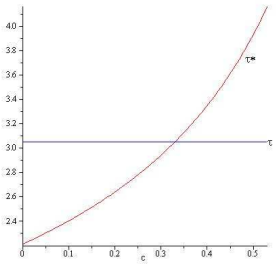

FIGURE 5. τ^* as a function of c with $K = 16, r = 0.52, \tau = 3.05$, and $I = 0.24$.

where N is a theoretical value, N_i is experimental value from the data, and we used weighted least squares with the weight being the normal probability density function applied annually (with $\sigma = 1$). The motivation behind such a choice of error function was to account for the fact that there are multiple zeros in the data. Figure 7(b) shows the model error as a function of two variables c and I.

From both Figure 7(a) and Figure 7(b) we see that the error function has a local minimum at $I = 0.24$ and $c = 0.35$. Figure 6 shows the theoretical fit (with optimal values of parameters) to the data.

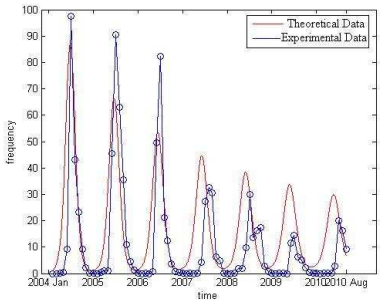

FIGURE 6. Theoretical fit vs experimental data

6. **Results and conclusions.** Edwards Plateau is an enormous region of Texas with over 20 vineyards and wineries distributed across this. Despite the large potential noise of different varieties, different age vineyards and viticultural techniques the GWSS insects population in this region were effectively modeled. There have been publications on the annual cycle of these insects for a region [19, 21]. However, the multi-year data set modeled here allowed us to model the decline in the population overtime. This decline correlates with an active campaign led to Texas AgriLife extension agents and scientists to help reduce the disease pressure introduced by GWSS. PD meetings throughout the early and mid 2000s urged growers to participate in several activities to reduce their threat of PD. Insect abundant activities included reduction of weeds on the vineyard floor, elimination of attractive host plants from around their vineyards and use of sharpshooter-specific insecticides

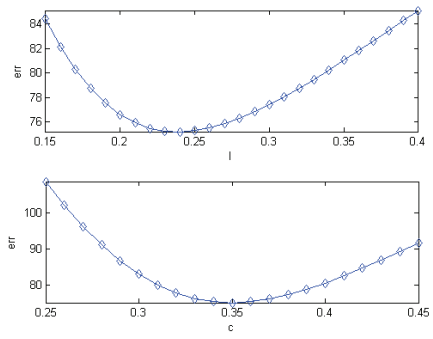

(a)

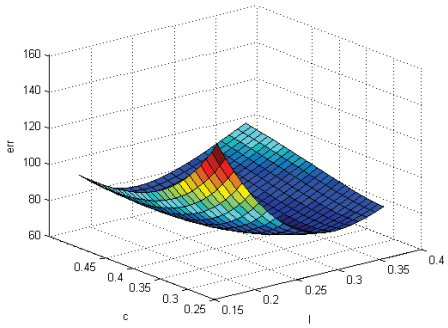

(b)

FIGURE 7. Model error as a function of c and I with $K = 16, r = 0.52$, and $\tau = 3.05$.

before the outbreak of GWSS adults in May [1]. It is also possible that changes in weather are the cause for the modeled population changes over multiple years. However, given that the insects prefer warm weather it would be more likely that warming of winters would have caused the populations to increase not decrease over time. It seems most reasonable that the harvesting term in this model is the result of viticultural interventions. This is valuable because it shows the time scale needed for such interventions to impact the large populations in a large geographic region. It also allows one to predict how long it takes before a population goes below an action threshold. Action threshold is a critical insect number used in integrated pest management to determine when an action must be taken to prevent an outbreak [8]. This model gives us the predictive power to determine the impact of human intervention on controlling a disease and to what minimal level (c^*) of intervention required. This model can also allow us to predict the increase in population over time if we were to stop controlling a disease (That is, remove c from the equation).

Our future plan in the modeling of this data is to consider an optimal control problem where the harvesting term would be a function of time. Another possible extension of the model is to include explicit representation of space in the model to

understand the impact of habitat heterogeneity and other spatial features on the management of the species.

Acknowledgments. This work is supported in part by NSF grant DUE-0734294, which enabled undergraduate students (Anh Tuan Nguyen and Sara Wilder) to participate in developing the mathematical model.

This material was made possible, in part, by a Cooperative Agreement from the United States Department of Agriculture's Animal and Plant Health Inspection Service (APHIS). It may not necessarily express APHIS' views.

REFERENCES

[1] R. Almeida, et al., Vector trasmission of *Xylella fastidiosa*: Applying fundamental knowledge to generate disease management strategies, *Ann. Entomol. Soc. Am.*, **98** (2005), 775–786.
[2] M. Begon, J. Harper and C. Townsend, *Ecology: Individuals, Populations and Communities*, 2nd edition, Blackwell Scientific Publications, Boston, MA, 1990.
[3] M. Blua, P. Philips,and R. A. Redak, A new sharpshooter threatens both crops and ornamentals, *Calif. Agr.*, **53** (1999), 22–25.
[4] S. Choi and N. Koo, Oscillation theory for delay and neutral differential equations, *Trends Math.*, **2** (1999), 170–176.
[5] D. R. Causton and J. C. Venus, *The Biometry of Plant Growth*, Edward Arnold, London, 1981.
[6] J. M. Cushing, *Integrodifferential Equations and Delay Models in Population Dynamics*, Lecture Notes in Biomathematics 20, Springer-Verlag, Heidelberg, 1977.
[7] J. De Leon, W. Joses and D. Morgan, Population genetic structure of *Homalodisca coagulata* (Homoptera: Cicadellidae), the vector of the bacterium *Xylella fastidiosa* causing Pierce's disease in grapevines, *Ann. Entomol. Soc. Am.*, **97** (2004), 809–818.
[8] http://www.epa.gov.
[9] W. W. Fox, An exponential surplus yield model for optimizing in exploited fish populations, *T. Am. Fish. Soc.*, **99** (1970), 80–88.
[10] K. Gopalsamy, *Stability and Oscillations in Delay Differential Equations of Population Dynamics*, Mathematics and its Applications 74, Kluwer Academic Publishers, Dordrecht, 1992.
[11] J. Grandgirard, G. Roderick, N. Davies, M. S. Hoddle and J. N. Petit, Engineering an invasion: Classical biological control of the glassy-winged sharpshooter, Homalodisca vitripennis, by the egg parasitoid Gonatocerus ashmeadi in Tahiti and Moorea, French Polynesia, *Biol. Invasions*, **10** (2008), 135–148.
[12] N. Hayes, Roots of the transcendendal equation associated with a certain differential difference equation, *J. London Math. Soc.*, **25** (1950), 226–232.
[13] W. Hewitt, The probable home of Pierce's disease virus, *Plant Dis. Rep.*, **42** (1958), 211–215.
[14] C. B. Hutchinson, Circular causal systems in ecology, *Ann. N.Y. Acad. Sci.*, **50** (1948), 221–246.
[15] http://www.ipm.ucdavis.edu.
[16] M. Kot, *Elements of Mathematical Ecology*, Cambridge University Press, 2001.
[17] R. Krugner, J. R. Hagler, J. G. Morse, A. P. Flores, R. L. Groves and M. W. Johnson, Seasonal population dynamics of Homalodisca vitripennis (Hemiptera: Cicadellidae) in sweet orange trees maintained under continuous deficit irrigation, *J. Econ. Entomol.*, **102** (2009), 960–973.
[18] Y. Kuang, *Delay Differential Equations with Applications in Population Dynamics*, Academic Press, New York, 1993.
[19] I. M. Lauzière, S. Sheather and F. L. Mitchell, Seasonal abundance and spatio-temporal distribution of dominant xylem fluid-feeding Hemiptera in vineyards of central Texas and surrounding habitats, *Environ. Entomol.*, **37** (2008), 925–937.
[20] N. MacDonald, *Time Lags in Biological Models*, Lecture Notes in Biomathematics 27, Springer-Verlag, Heidelberg, 1978.
[21] F. L. Mitchell, J. Brady, B. Bextine and I. M. Lauzière, Seasonal increase of *Xylella fastidiosa* in Hemiptera collected from central Texas vineyards, *J. Econ. Entomol.*, **102** (2009), 1743–1749.

[22] L. Morano, J. Yoon, A. Abedi and F. Mitchell, Evaluation of xylem-feeding insects (Hemiptera: Auchennorrhyncha) in Texas vineyards: distribution along state-wide environmental gradients, *Southwest. Entomol.*, **35** (2010), 503–512.
[23] R. Redak, et al., The biology of xylem fluid-feeding insect vectors of *Xylella fastidiosa* and their relation to disease epidemiology, *Annu. Rev. Entomol.*, **49** (2004), 243–270.
[24] S. Ruan, Delay differential equations in single species dynamics, in *Delay Differential Equations and Applications* (eds. O. Arino et al.), Springer, Berlin, 2006, 477–517.
[25] M. Setamou and W. A. Jones, Biology and biometry of sharpshooter *Homalodisca coagulata* (Homoptera: Cicadellidae) reared on cowpea, *Ann. Entomol. Soc. Am.*, **98** (2005), 322–328.
[26] J. Maynard Smith, *Models in Ecology*, Cambridge University Press, 1974.
[27] Hal Smith, *An Introduction to Delay Differential Equations with Applications to the Life Sciences*, Springer, 2011.
[28] D. Takiya, S. McKamey and R. Cavichioli, Validity of *Homalodisca* and of *H. vitripennis* as the name for glassy-winged sharpshooter (Hemiptera: Cicadellidae), *Ann. Entomol. Soc. Am.*, **99** (2006), 648–655.
[29] T. E. Wheldon, *Mathematical Models in Cancer Research*, Adam Hilger, Bristol, 1988.
[30] E. M. Wright, The non-linear difference-differential equation, *Q. J. Math.*, **17** (1946), 245–252.

Received January 14, 2013; Accepted July 27, 2013.

E-mail address: YoonJ@uhd.edu
E-mail address: HrynkivV@uhd.edu
E-mail address: MoranoL@uhd.edu
E-mail address: nguyena48@gator.uhd.edu
E-mail address: wilders1@gator.uhd.edu
E-mail address: f-mitchell@tamu.edu